

Conformationally locked thiosugars as potent α -mannosidase inhibitors: Synthesis, biochemical and docking studies

K. Sivapriya,^a S. Hariharaputran,^b V. L. Suhas,^b N. Chandra^b and S. Chandrasekaran^{a,*}

^aDepartment of Organic Chemistry, Indian Institute of Science, Bangalore, Karnataka 560012, India

^bBioinformatics Centre, Supercomputer Education & Research Centre, Indian Institute of Science, Bangalore, Karnataka 560012, India

Received 15 May 2007; revised 3 June 2007; accepted 5 June 2007

Available online 8 June 2007

Abstract—A series of thiosugar derivatives (thiolevomannosans) derived from mannose were synthesized and their inhibitory activity was tested against α -mannosidase (jack bean). These inhibitors were found to be more potent than the well-known inhibitors like kifunensine and deoxymannojirimycin based on docking and biochemical studies. The sulfone derivative **10** was shown to be the best inhibitor of α -mannosidase with the K_i value of 350 nM.

© 2007 Elsevier Ltd. All rights reserved.

1. Introduction

α -Mannosidase, a member of the ‘processing glycosidases’ in the human endoplasmic reticulum, is important for the biosynthesis of several glycoproteins, due to its ability to process *N*-glycans by trimming $\text{Glc}_3\text{Man}_9\text{GlcNAc}_2$ moieties. $\text{Glc}_3\text{Man}_9\text{GlcNAc}_2$ then undergoes trimming of the glucose and some of the mannose residues, first in the ER and then in the Golgi, followed by the addition of branching *N*-acetyl glucosamine and additional sugars, such as galactose, fucose, and sialic acid by Golgi glycosyl transferase to form hybrid and complex *N*-glycans.¹

Compounds that selectively inhibit these glycosidases have attracted interest because of the significance of such inhibition to both viral expression and tumor growth. α -Mannosidases remove mannose residues from the maturing oligosaccharide by hydrolyzing the mannosyl glycosidic bond. The trimming of a single mannose at this step is a targeting signal for translocation out of the ER to proteasome for degradation. Because mannosidase inhibitors block degradation of misfolded glycoproteins, it has been suggested that the

removal of mannose units by α -mannosidase might work as the timer for glycoprotein degradation.²

Of the numerous classes of inhibitors reported, an aza sugar, kifunensine **2** (Fig. 1), is one of the most potent and promising.^{3a} However, synthesis of its enantiomerically pure form involves many steps and still remains a challenge.⁴

Mannose **4** in solution or as a part of an oligosaccharide exists predominantly in the 4C_1 conformation. However, the existing inhibitors (**2** and **3**) adopt the unfavorable, axial rich 1C_4 chair conformation in the active site of the enzyme^{3a,b} and this conformation is stabilized through hydrogen bonding and hydrophobic interactions. In kifunensine **2** the presence of a fused five-membered ring facilitates 1C_4 conformation and is stabilized by calcium ion coordination.⁵ Recently Boons et al. have reported the existence of different conformations of an inhibitor in the free state while it exists as a single conformer when bound to the enzyme.⁶ Conformational locking of the groups is therefore an obvious rationale for the design of promising pharmacophoric drug candidates. This prompted us to study the synthesis and evaluation of the inhibition of α -mannosidase by conformationally locked thiosugars of the type **1** and its derivatives (Scheme 1).

Keywords: Thiosugars; Inhibition; α -Mannosidase; Docking studies.

* Corresponding author. E-mail: scn@orgchem.iisc.ernet.in

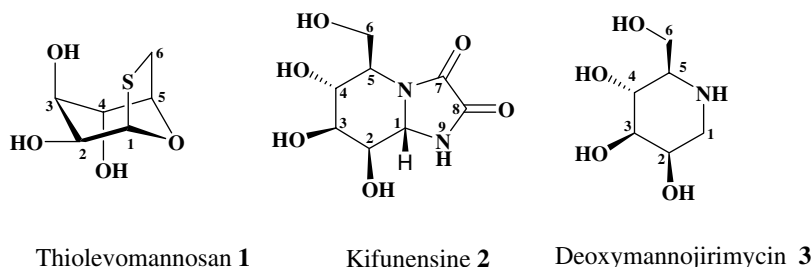
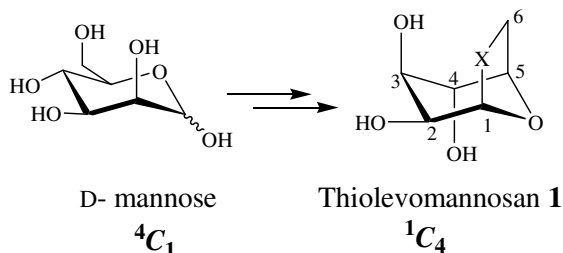


Figure 1.

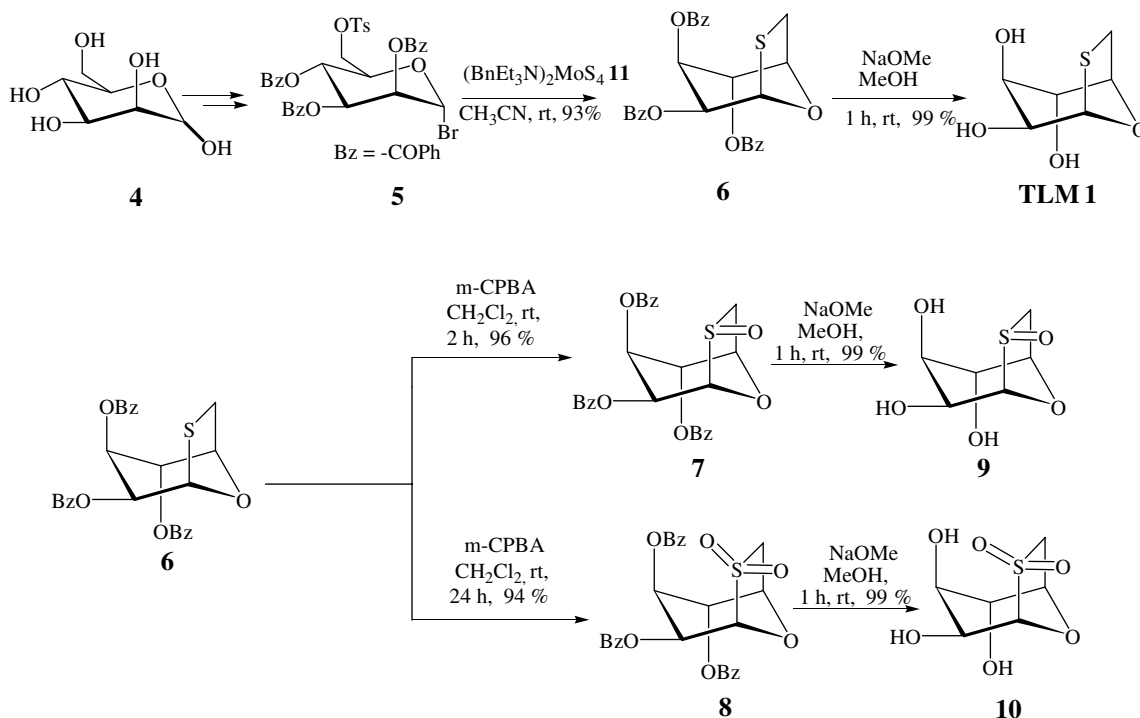


Scheme 1.

Herein, we report the synthesis and evaluation of novel, conformationally locked glycomimic thiolevomannosan (TLM) **1** and its analogs **9** and **10** starting from readily available D-mannose. This is the first report of thiosugar derivatives with enhanced potency compared to kifunensine **2** as evidenced by docking studies of the protein–**1** complex as well as biochemical studies.

2. Chemistry

Recently we reported an efficient and facile synthesis of a number of thiolevomannosan derivatives in good yields.⁷ Thiolevomannosan **1** was synthesized from D-mannose **4**, in four steps in high yield (Scheme 2). Mannosyl bromide **5**, on treatment with benzyldiethylammonium tetrathiomolybdate, $(\text{BnEt}_3\text{N})_2\text{MoS}_4$ **11**,⁸ gave the benzoyl protected thiosugar **6**⁷ (93%). Hydrolysis of compound **6** with NaOMe/MeOH (1 h, 28 °C) furnished the required thiolevomannosan **1** (TLM) in 99% yield. Compound **1** was fully characterized by spectroscopy and the conformationally locked, axial rich structure was confirmed by X-ray crystallography (Fig. 2). When **6** was oxidized using *m*-CPBA (CH_2Cl_2 , 2 h, 28 °C) it led to the formation of sulfoxide **7** in 96% yield. When the reaction of **6** with excess *m*-CPBA was carried out for a longer period (24 h) the corresponding sulfone **8** was formed in 94% yield. Hydrolysis of **7** and **8** using NaOMe/MeOH (1 h, 28 °C) furnished **9** (XLM) and **10** (NLM), respectively, in high yields (99%). The conform-



Scheme 2.

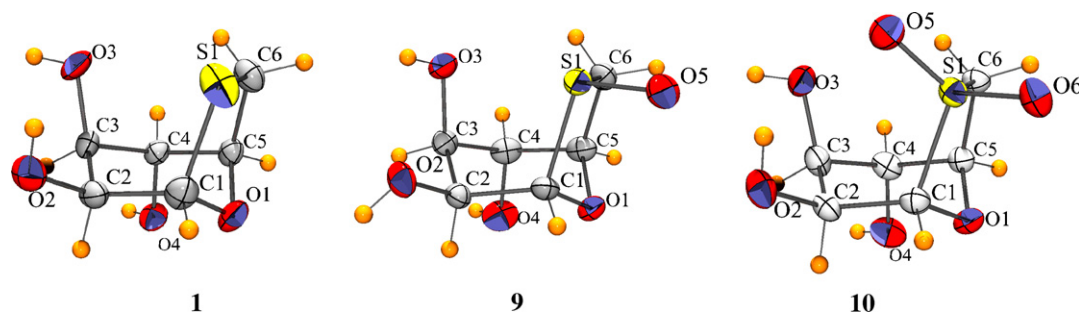


Figure 2. ORTEP diagrams of **1**, **9**, and **10**.

ationally locked, axial rich structures of **9** and **10** were also confirmed by X-ray studies (Fig. 2).

3. Docking studies

The crystal structure of human α -1,2-mannosidase complexed with kifunensine (PDB: 1FO3) was used as a template for the docking studies. The protein coordinates

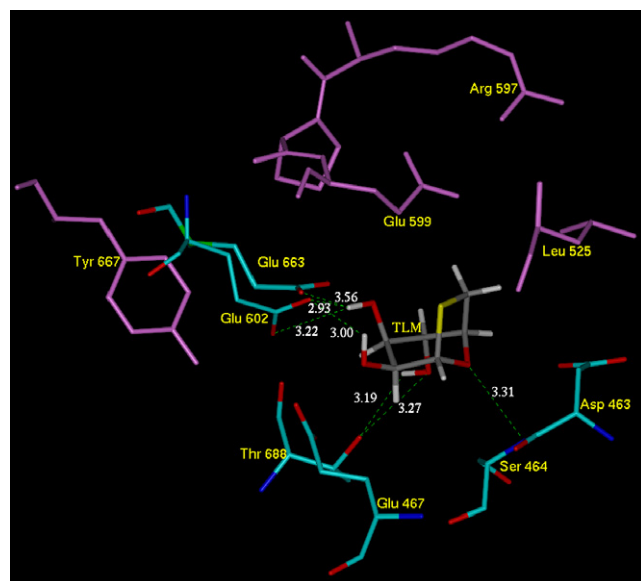


Figure 3. Binding of TLM **1** to mannosidase active pocket. Broken lines indicate hydrogen bonds. A docking grid of 60 Å³ (0.375 spacing) was computed around the binding site of apo-mannosidase (PDB: 1FO3). TLM **1** placed in different locations outside the grid consistently docked well into the binding site. (As estimated by Autodock runs using 3,750,000 energy evaluations over 150 GA runs).

from the structure were used to dock thiolevo-mannosan (TLM) **1** into the binding site which was then subjected to energy minimization using DISCOVER module interfaced with Insight II suite.⁹ The docking was carried out by the Autodock algorithm.¹⁰ The interactions between the ligand **1** and the protein were assessed by measuring hydrogen bonds. Distances between polar atoms less than 3.6 Å were regarded as hydrogen bonds. A genetic-algorithm based docking study (Autodock) carried out to understand the feasibility and mode of binding to human α -1,2-mannosidase indicates that TLM **1** binds at the same active pocket of the enzyme where the other inhibitors bind⁵ (Fig. 3). A positive control with kifunensine **2** gave the expected results. TLM **1** makes seven hydrogen bonds, of which six are through its O2 and O3 hydroxyls and additional hydrogen bonds through O1 and O4 (Fig. 3 and Table 1). Kifunensine **2** on the other hand, although binding at the same overall location, makes mainly water mediated interactions through O2 and O3 hydroxyls and requires co-ordination through calcium. Water and calcium in turn interact with the catalytic residues.⁵

The active site mainly consists of glutamate residues that make the site very acidic. The residues which are not interacting with the ligand **1** are depicted in purple (Fig. 3). With **1**, except Glu 599 the other glutamate residues form strong hydrogen bonds which are well within the limits (3.6 Å). Binding of sulfoxide **9** and sulfone **10** to mannosidase active pocket is presented in Figures 4 and 5, respectively. There are a few catalytic amino acid residues like Glu-602 and Ser-464 which bind to all the three ligands. Glu-599 forms hydrogen bonds with both thiolevo-mannosan **1** and sulfoxide derivative **9**. The residues of α -mannosidase involved in hydrogen bonding with all the ligands including kifunensine are given in Table 1.

Table 1. Hydrogen bond interactions: active site residues of α -mannosidase with the ligands

Interacting atom of the ligand	TLM 1	XLM 9	NLM 10	Kif 2
O1	Ser-464	Thr-688	—	—
O2	Glu-602, Glu-467	Glu-602, Glu-467	Asp-463	Thr-688
O3	Glu-663 Glu-602	Glu-599 Glu-602	Glu-689, Thr-688	Glu-663
O4	Thr-688	Glu-663, Glu-663, Thr-688	Glu-663	Glu-689
O5	Asp-463	Asp-463	Thr-688, Glu-467, Ser-464, Asp-463	—
O6	—	—	Glu-467	Arg-597, Glu-599
O7	—	—	—	Arg-597
N9	—	—	—	Asp-463

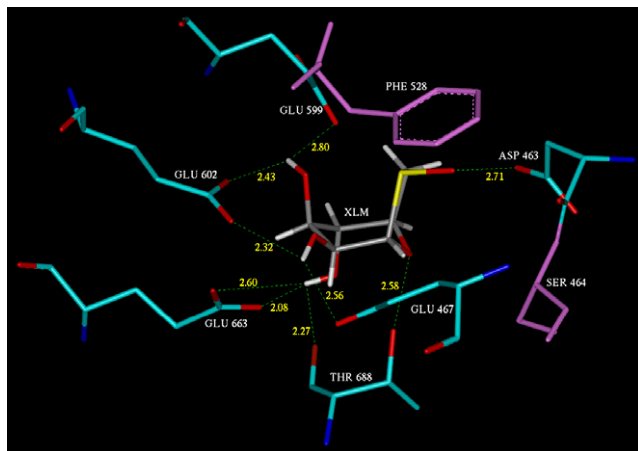


Figure 4. Binding of sulfoxide **9** to mannosidase (PDB: 1FO3) active pocket.

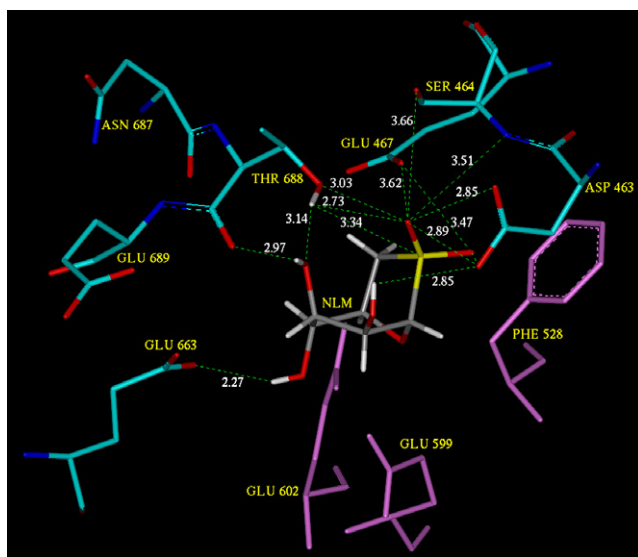


Figure 5. Binding of sulfone **10** (bottom) to mannosidase (PDB: 1FO3) active pocket.

Kifunensine forms strong hydrogen bonds with Arg-597 and Arg-334. But these residues do not have any interactions with the other ligands **1**, **9**, and **10**. Glu-689 interacts with both kifunensine **2** as well as with **10**. Asp-463 forms hydrogen bond with **2**, **9**, and **10** but not with **1**. Only Thr-688 is a common residue that has interactions with all the ligands **1**, **2**, **9**, and **10**. Kifunensine forms totally nine hydrogen bonds with the active site residues as that of the sulfoxide **9**, but the sulfone **10** forms the maximum number of hydrogen bonds (total 13) with the active site residues suggesting that the sulfone **10** is

much more strongly bound to the active pocket of the enzyme.

Interactions less than 4.5 Å are taken as van der Waals interactions. The residues involved in van der Waals interactions are given in Table 2. Ser-464 is the only residue that has weak interaction with all the three ligands (**1**, **9**, and **10**). The only van der Waals interactions found in kifunensine **2** are with Phe-659 and Leu-525.⁵

Figure 6a shows the superimposed picture of **1**, **9**, and **10** over kifunensine **2**. All the ligands superimpose very well with kifunensine **2**. Figure 6b shows the docking picture of all the ligands inside the active site of the enzyme. Sulfoxide **9** (XLM) docks the same way as that of TLM **1** but the sulfone derivative **10** (NLM) docks differently where the sulfone group can make more number of hydrogen bonds with the catalytic residues. The binding energy values and shape complementarity values of all the ligands are given in Table 3.

4. Biological studies

Inhibition analysis was done using sodium acetate buffer (pH 4.5). Enzymatic activity was determined by spectrophotometric method at 405 nm for α -mannosidase (jack bean) using *p*-nitrophenyl α -D-mannopyranoside as the substrate. The complete sequence of jack bean mannosidase is yet to be reported. Therefore it is difficult to compare the active sites of the mannosidase from jack bean and ER. It is expected that the two enzymes will have different specificity. Since jack bean α -mannosidase is commercially available and may provide a convenient model system¹¹ for the more valuable mammalian enzymes, it has been used for the biochemical studies.

The inhibition constant (K_i) values (for jack bean mannosidase) are given in Table 4. It shows that the sulfone **10** (NLM) is a more potent inhibitor than **1** (TLM) and **9** (XLM). The stronger binding of **1** is also reflected by higher shape complementarity (0.736 for **1**, 0.707 for **9** and 0.737 for **10** vs 0.636 for **2**) computed following a post-docking energy minimization.⁹ The values of shape complementarity for the other ligands **9** and **10** are given in Table 3. This observation is corroborated by enzymatic assays of inhibition constant of 1.38 μ M for TLM **1**, 385 nM for **9**, and 350 nM for **10** (Table 4).

5. Conclusion

In summary, the syntheses of **1**, **9**, and **10** are simple and high-yielding, giving conformationally locked thiosugars in a few steps. These ligands with a stable ¹C₄ conformation have an advantage over other inhibitors, since they have the required conformation for presentation to the active site of the enzyme. Docking studies show stronger binding of **1**, **9**, and **10** over kifunensine **2**. Thiolevomannosan **1** and its analogs **9** and **10** serve as a framework to design and synthesize different analogs that can lead to the discovery of drugs that are potent mannosidase inhibitors.

Table 2. Residues involved in van der Waals interactions

Ligand	Interacting residues
TLM 1	Ser-464, Leu-525, Pro-598, Glu-689
XLM 9	Pro-598, Glu-689, Ser-464
NLM 10	Ser-464
Kif 2	Phe-659, Leu-525

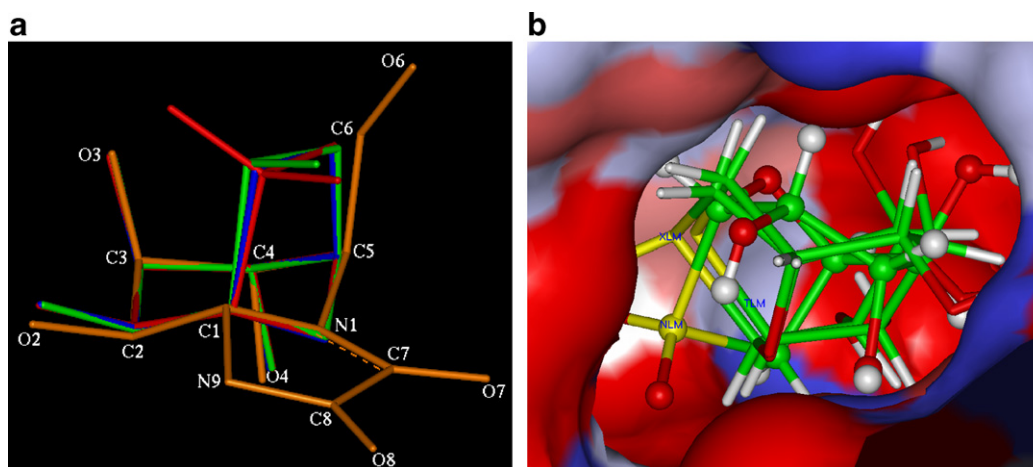


Figure 6. (a) Superimposed picture of KIF-2, TLM-1, XLM 9, and NLM 10. Orange-kifunensine (KIF), blue-thiolevomannosan (TLM 1), Green-sulfoxide 9 (XLM), red-sulfone 10 (NLM). (b) Active site of human α -mannosidase (9 Å) with all the above inhibitors superimposed.

Table 3. Binding energy values of the ligands

Ligand	Shape complementarity	Final docked energy (kcal/mol) ^a	Intermolecular energy upon minimization of the complex ^b
Kif	0.636	−8.10	−27.7
TLM	0.736	−7.59	−37.3
XLM	0.707	−7.27	−58.7
NLM	0.737	−7.29	−63.7

^a The values obtained by using Autodock, Amber.

^b Discover, and Insight II.

Table 4. Inhibition constant of the inhibitors

Compound	K_i
TLM 1	1.38 μ M
XLM 9	385 nM
NLM 10	350 nM
Kif 2	Not reported
DMJ 3	400 μ M ¹²

6. Experimental

6.1. General methods

Melting points were recorded on a BUCHI B540 melting point apparatus and are uncorrected. ^1H and ^{13}C NMR spectra were recorded on a JEOL—400 and 75 MHz spectrometer, respectively. Chemical shifts are reported in parts per million downfield from the internal reference, tetramethylsilane. Coupling constants are reported wherever necessary in Hertz (Hz). Flash column chromatography was performed on silica gel (230–400 mesh). Mass spectra were recorded on a Q-TOF electrospray instrument. Data collections were recorded on a BRUKER-SMART APEX CCD—single crystal diffractometer. Inhibition analyses were done using sodium acetate buffer (pH 4.5). Enzymatic activity was determined by spectrophotometric method (SHIMADZU 160A UV–visible spectrometer) at 405 nm for α -mannosidase (jack bean from Sigma–Aldrich) using *p*-nitrophenyl α -D-mannopyranoside as the substrate.

6.2. General procedure for the synthesis of 7 and 8

6.2.1. Synthesis of 2,3,4-tri-*O*-benzoyl-1,6-dideoxy-1,6-episulfinyl- β -D-mannose (7). To a solution of **6**⁷ (0.2 g, 0.41 mmol) in CH_2Cl_2 (2 ml), *m*-CPBA (0.19 g, 1.02 mol) was added at room temperature (28 °C) and stirred for 2 h. The reaction mixture was then washed with saturated sodium sulfite solution (2 \times 20 ml) to remove the excess acid formed in the reaction and then with water (2 \times 25 ml), the organic layer was dried over anhydrous sodium sulfate, and the filtrate was concentrated to give the crude product which on purification by flash column chromatography on silica gel (230–400 mesh) eluting with hexane/ethyl acetate 4:6 furnish compound sulfoxide **7** as a white solid (0.19 g, 96%).

6.2.2. Synthesis of 2,3,4-tri-*O*-benzoyl-1,6-dideoxy-1,6-episulfonyl- β -D-mannose (8). To a solution of **6** (0.2 g, 0.41 mmol) in CH_2Cl_2 (2 ml), *m*-CPBA (0.38 g, 2.04) was added at room temperature (28 °C) and stirred for 2 h. After the reaction the work-up procedure described in Section 6.2.1 was followed to obtain the sulfone **8** (0.2 g, 94%) as a white gummy solid.

6.2.3. 2,3,4-Tri-*O*-benzoyl-1,6-dideoxy-1,6-episulfinyl- β -D-mannose (7). Mp 111 °C; ^1H NMR (300 MHz, CDCl_3): δ 8.15–7.26 (15H, aromatic), 5.86 (t, 1H, J = 4.8 Hz), 5.77–5.74 (m, 1H), 5.56 (d, 1H, J = 4.2 Hz), 5.48 (d, 1H, J = 8.1 Hz), 5.13 (t, 1H, J = 1.8 Hz), 4.30 (d, 1H, J = 12.9 Hz), 3.06 (dd, 1H, J_1 = 8.4 Hz, J_2 = 13.2 Hz); ^{13}C NMR (75 MHz, CDCl_3): δ 164.9, 164.6, 164.4, 134.2, 134.0, 133.9, 130.1, 129.9, 129.8, 128.9, 128.7, 128.5, 128.2, 100.6, 78.6, 70.6, 67.5, 66.3, 59.9; HRMS (m/z): Calculated for $\text{C}_{27}\text{H}_{22}\text{O}_8\text{S}$ ($\text{M}+\text{Na}^+$): 529.0933, Observed ($\text{M}+\text{Na}^+$): 529.0943.

6.2.4. 2,3,4-Tri-*O*-benzoyl-1,6-dideoxy-1,6-episulfonyl- β -D-mannose (8). ^1H NMR (300 MHz, CDCl_3): δ 7.75–7.29 (15H, aromatic), 4.81 (dd, 1H, J_1 = 9.3 Hz, J_2 = 1.2 Hz); 4.23 (t, J = 4.8 Hz, 1H), 4.0 (s, 1H), 3.91 (s, 1H), 3.66 (dd, 1H, J_1 = 2.1 Hz, J_2 = 13.2 Hz), 3.39–3.31 (m, 1H); HRMS (m/z): Calculated for $\text{C}_{27}\text{H}_{22}\text{O}_9\text{S}$ ($\text{M}+\text{Na}^+$): 545.0882, Observed ($\text{M}+\text{Na}^+$): 545.0776.

6.3. General procedure for the synthesis of **1**, **9**, and **10**

6.3.1. Typical procedure for the synthesis of 1,6-dideoxy-1,6-epithio- β -D-mannose (1**).** To a stirred solution of **6** (0.18 g, 0.366 mmol) in dry methanol (2 ml) was added a methanolic solution of sodium methoxide (prepared by dissolving 50 mg of sodium in 2 ml methanol), and the solution was stirred for 1 h at 28 °C. The reaction mixture was acidified (pH 5) with Amberlite (H⁺) IR-120 resin. After filtering the resin the solvent was evaporated and the residue was purified by flash column chromatography on silica gel (230–400 mesh, eluting with methanol/chloroform, 1:9) to get a colorless solid, which was recrystallized from methanol to furnish shiny crystals of **1** (0.065 g, 99%).

6.3.2. 1,6-Dideoxy-1,6-epithio- β -D-mannose (1**).** $[\alpha]_D^{25}$ –117 (*c* 1, CH₃OH)¹³ mp 259 °C; ¹H NMR (400 MHz, CD₃OD): δ 5.29 (d, 1H, *J* = 0.96 Hz), 4.71 (dd, 1H, *J* = 1.5 Hz), 4.20 (t, 1H, *J* = 12.7 Hz), 3.79 (dd, 1H, *J* = 10.9 Hz), 3.71 (dd, 2H, *J* = 1.72 Hz), 3.34 (m, 2H); ¹³C NMR (75 MHz, CD₃OD): 84.5, 80.0, 73.1, 70.8, 64.9, 48.2, 48.0, 47.9, 47.6, 47.4, 47.2, 46.9, and 31.7; HRMS: Calculated mass for C₆H₁₀O₄S: 201.0198, Observed (M+Na⁺): 201.0193.

6.3.3. 1,6-Dideoxy-1,6-episulfinyl- β -D-mannose (9**).** Yield: 99%; $[\alpha]_D^{25}$ 18 (*c* 1, H₂O) mp 180 °C; ¹H NMR (400 MHz, D₂O): δ 5.16 (d, 1H, *J* = 4.1 Hz), 5.04 (d, 1H, *J* = 8.0 Hz), 4.17–4.14 (m, 2H), 3.78 (br s, 1H), 3.67 (br s, 1H), 2.64 (dd, 1H, *J*₁ = 8.2 Hz, *J*₂ = 13.9 Hz); ¹³C NMR (75 MHz, D₂O): 103.5, 80.8, 69.8, 69.7, 66.3 and 59.2; HRMS: Calculated mass for C₆H₁₀O₅S: 217.0147, Observed (M+Na⁺): 217.0147.

6.3.4. 1,6-Dideoxy-1,6-episulfonyl- β -D-mannose (10**).** Yield: 99%; $[\alpha]_D^{25}$ 7 (*c* 1, H₂O) mp 213 °C; ¹H NMR (300 MHz, CD₃OD): δ 4.77 (bd, 1H, *J* = 9.3 Hz), 4.5 (bd, 1H, *J* = 4.5 Hz), 4.23 (t, 1H, *J* = 5.1 Hz), 4.0–3.98 (m, 1H), 3.87 (br s, 1H), 3.70 (td, 1H, *J*₁ = 12.6 Hz, *J*₂ = 12.6 Hz), 3.34–3.21 (m, 1H); ¹³C NMR (75 MHz, CD₃OD): 87.4, 78.5, 72.7, 71.6, 67.4, and 33.0; HRMS: Calculated mass for C₆H₁₀O₆S: 233.0096, Observed (M+Na⁺): 233.0117.

6.4. Crystal structure data for (**1**)

CCDC 260886: C₆H₁₀O₄S, Mwt = 178.2, Crystal dimensions 0.30 × 0.25 × 0.20, *T* = 293(2) K, Orthorhombic, Space group P 21 21 21, *a* = 5.9869(10), *b* = 9.9287(17), *c* = 12.160(2) Å, $\alpha = \beta = \gamma = 90.00^\circ$, *Z* = 4, *V* = 722.8(2) cm³, $\rho_{\text{calcd}} = 1.64 \text{ g/cm}^3$, MoK α radiation ($\lambda^\circ = 0.71073 \text{ Å}$), $\mu = 4.08 \text{ mm}^{-1}$, $2\theta = 2.65$ – 27.82° ; of 5903 reflections collected, 1604 were independent (*R* (int) = 0.0247); refinement method full matrix least squares on *F*₂, 141 refined parameters, absorption correction (SADABS, Bruker, 1996 software, *T*_{min} 0.8874 and *T*_{max} 0.9229), GOF = 1.098, *R*₁ = 0.0241, *wR*₂ = 0.0636 ($\sigma > 2\sigma(\text{I})$), absolute structure parameter 0.00(7), residual electron density 0.221/–0.135 eÅ^{–3}. The structure was solved and refined with the programs WinGXv1.64.05, Sir92, and SHELXL-97.

6.5. Crystal structure data for (**9**)

CCDC 618881: C₆H₁₀O₅S, Mwt = 194.20, Crystal dimensions 0.5 × 0.5 × 0.5 mm³, *T* = 293(2) K, Monoclinic, Space group P 21, *a* = 5.5194(11), *b* = 10.834(2), *c* = 6.5168(13) Å, $\alpha = \gamma = 90.00^\circ$, $\beta = 96.842(3)^\circ$, *Z* = 2, *V* = 386.90(13) cm³, $\rho_{\text{calcd}} = 1.667 \text{ Mg/m}^3$, MoK α radiation ($\lambda^\circ = 0.71073 \text{ Å}$), $\mu = 0.398 \text{ mm}^{-1}$, $2\theta = 3.15$ – 25.99° ; of 2995 reflections collected, 1498 were independent (*R* (int) = 0.0149); refinement method full matrix least squares on *F*₂, 141 refined parameters, absorption correction (SADABS, Bruker, 1996 software), GOF = 1.070, *R*₁ = 0.0261, *wR*₂ = 0.0651 ($\sigma > 2 \sigma(\text{I})$), absolute structure parameter 0.04(7), residual electron density 0.225 and –0.187 eÅ^{–3}.

6.6. Crystal structure data for (**10**)

CCDC 618882: C₆H₁₀O₆S_{0.5}, Mwt = 194.17, Crystal dimensions 0.5 × 0.47 × 0.36 mm³, *T* = 293(2) K, Orthorhombic, Space group P 21 21 21, *a* = 6.884(2), *b* = 9.325(3), *c* = 11.874(4) Å, $\alpha = \gamma = \beta = 90.00^\circ$, *Z* = 4, *V* = 762.2(4) cm³, $\rho_{\text{calcd}} = 1.692 \text{ Mg/m}^3$, MoK α radiation ($\lambda^\circ = 0.71073 \text{ Å}$), $\mu = 0.281 \text{ mm}^{-1}$, $2\theta = 2.78$ – 26° ; of 4313 reflections collected, 1513 were independent (*R* (int) = 0.0213); refinement method full matrix least squares on *F*₂, 141 refined parameters, absorption correction (SADABS, Bruker, 1996 software), GOF = 1.099, *R*₁ = 0.0301, *wR*₂ = 0.0731 ($\sigma > 2 \sigma(\text{I})$), absolute structure parameter –0.01(9), residual electron density 0.282 and –0.202 eÅ^{–3}.

The structures were solved and refined with the programs WinGXv1.64.05, Sir92, and SHELXL-97. Crystallographic data for the above compounds **1**, **9**, and **10** have been deposited with the Cambridge crystallographic data centre. Copies of the data can be obtained free of charge on application to CCDC, 12 Union Road, Cambridge, CB2 1EZ, UK, +44 1223 336408; email: deposit@ccdc.cam.ac.uk.

6.7. Procedure for biochemical assays

The enzyme and the inhibitor in buffer solution (sodium acetate, pH 4.5) were incubated at 35 °C for 15 min. Then the corresponding substrate (*p*-nitrophenyl α -D-mannopyranoside) was added and the solution was again incubated for 45 min. After this a saturated solution of sodium carbonate was added to stop the reaction. Then the OD measurements have been taken in triplets at 405 nm. The precise *K*_i value was derived from nonlinear least-squares fits of the data and the double reciprocal analysis (Dixon plot) established that the inhibitor was competitive.

Acknowledgments

The authors thank DST, New Delhi, for CCD X-ray facility and Vijay Thiruvengatam for help in solving the molecular structures **1**, **9**, and **10**. We thank Dr. Ian Beadham for valuable discussions. We also thank Dr. Utpal Tatu and Prof. Anjali Karande, Department

of Biochemistry, for providing the laboratory facilities for enzymatic assay experiments and for valuable discussions. Use of facilities at SERC, DBT supported Bioinformatics Centre and Interactive Graphics facility is gratefully acknowledged.

References and notes

1. Herscovics, A. *Biochim. Biophys. Acta* **1999**, *1473*, 96–107.
2. Ellgaard, L.; Molinari, M.; Helenius, A. *Science* **1999**, *286*, 1882–1888.
3. (a) Shah, N.; Kuntz, D. A.; Rose, D. R. *Biochemistry* **2003**, *42*, 13812–13816; (b) Vasella, A.; Davies, G. J.; Böhm, M. *Curr. Opin. Chem. Biol.* **2002**, *6*, 619–629.
4. Hudlicky, T.; Rouden, J.; Luna, H.; Allen, S. *J. Am. Chem. Soc.* **1994**, *116*, 5099–5107.
5. Vallee, F.; Karaveg, K.; Herscovics, A.; Moremen, K. W.; Howell, P. L. *J. Biol. Chem.* **2000**, *275*, 41287–41298.
6. Kawatkar, S. P.; Kuntz, D. A.; Woods, R. J.; Rose, D. R.; Boons, G.-J. *J. Am. Chem. Soc.* **2006**, *128*, 8310–8319.
7. Sivapriya, K.; Chandrasekaran, S. *Carbohydr. Res.* **2006**, *341*, 2204–2210.
8. Prabhu, K. R.; Devan, M. N.; Chandrasekaran, S. *Synlett* **2002**, 1762–1778.
9. www.accelrys.com.
10. Morris, G. M.; Goodsell, D. S.; Halliday, R. S.; Huey, R. W. E.; Belew, R. K.; Olson, A. J. *J. Comput. Chem.* **1998**, *19*, 1639–1662.
11. Howard, S.; Braun, C.; McCarter, J.; Moremen, K. W.; Liao, Y.-F.; Withers, S. G. *Biochim. Biophys. Res. Commun.* **1997**, *238*, 896–898.
12. Legler, G.; Julich, E. *Carbohydr. Res.* **1984**, *128*, 61–72.
13. Chu, C. K.; Beach, J. W.; Jeong, L. S.; Choi, B. G.; Comer, F. I.; Alves, A. J.; Schinaz, R. F. *J. Org. Chem.* **1991**, *56*, 6503–6505.